

## Measurement of the Reaction ${}^2\text{H}(e, e')$ at $180^\circ$ Close to the Deuteron Breakup Threshold

N. Ryezayeva,<sup>1,\*</sup> H. Arenhövel,<sup>2</sup> O. Burda,<sup>1</sup> A. Byelikov,<sup>1</sup> M. Chernykh,<sup>1</sup> J. Enders,<sup>1</sup> H. W. Griebhammer,<sup>3</sup> Y. Kalmykov,<sup>1</sup> P. von Neumann-Cosel,<sup>1,†</sup> B. Özcel,<sup>1,4</sup> I. Poltoratska,<sup>1</sup> I. Pysmenetska,<sup>1</sup> C. Rangacharyulu,<sup>5</sup> S. Rathi,<sup>1</sup> A. Richter,<sup>1</sup> G. Schrieder,<sup>1</sup> A. Shevchenko,<sup>1</sup> and O. Yevetska<sup>1</sup>

<sup>1</sup>*Institut für Kernphysik, Technische Universität Darmstadt, D-64289 Darmstadt, Germany*

<sup>2</sup>*Institut für Kernphysik, Universität Mainz, D-55099 Mainz, Germany*

<sup>3</sup>*Center for Nuclear Studies, Department of Physics, George Washington University, Washington, D.C. 20052, USA*

<sup>4</sup>*Science and Art Faculty, Çukurova University, 01330 Adana, Turkey*

<sup>5</sup>*Department of Physics, University of Saskatchewan, Saskatoon, Canada, S7N 5E2*

(Received 10 December 2007; published 28 April 2008)

Inclusive inelastic electron scattering off the deuteron under  $180^\circ$  has been studied at the S-DALINAC close to the breakup threshold at momentum transfers  $q = 0.27 \text{ fm}^{-1}$  and  $0.74 \text{ fm}^{-1}$  with good energy resolution sufficient to map in detail the spin flip  $M1$  response, which governs the starting reaction  $pn \rightarrow d\gamma$  of big-bang nucleosynthesis over most of the relevant temperature region. Results from potential model calculations and (for  $q = 0.27 \text{ fm}^{-1}$ ) from pionless nuclear effective field theory are in excellent agreement with the data.

DOI: [10.1103/PhysRevLett.100.172501](https://doi.org/10.1103/PhysRevLett.100.172501)

PACS numbers: 25.30.Fj, 21.45.-v, 26.35.+c, 27.10.+h

Breakup of the deuteron as the simplest composite nuclear system in electromagnetic reactions is a classical tool to study elementary properties of the nucleon-nucleon interaction [1]. Current models based on meson-exchange potentials are expected to provide a successful description at low energies and momentum transfers (see, e.g., Ref. [2] and references therein). There is renewed interest in such data in view of the recent development of nuclear effective field theories (EFTs) (see, e.g., Refs. [3,4] for recent reviews). The fiducial domain of its “pionless” version discussed here—called EFT( $\not{\pi}$ )—is constrained to momentum transfers small compared to the inverse range of the pion-exchange potential.

Because of its role in big-bang nucleosynthesis (BBN) of the lightest stable isotopes  ${}^2\text{H}$ ,  ${}^3,{}^4\text{He}$ , and  ${}^7\text{Li}$ , a particularly interesting case is a detailed measurement of the spin flip  $M1$  resonance dominating the response just above the breakup threshold. At typical BBN temperatures [5] the light-element abundances are influenced by the  $pn \rightarrow d\gamma$  reaction for energies of about 20 to 200 keV in the center-of-mass system, i.e., in the region of the  $M1$  resonance. Data for this reaction [6], or data extracted from the inverse  $\gamma d \rightarrow pn$  reaction [7–11] by the principle of detailed balance, are scarce and show unsatisfactory scattering. As a result, the uncertainties of the data induce similar substantial uncertainties of the extracted abundances, especially for  ${}^2\text{H}$  and  ${}^7\text{Li}$  [5,12,13]. Their reduction is of considerable importance in light of a recent determination of the only free parameter of the standard model of BBN, viz. the baryonic density, through high-precision measurements of the anisotropy of the cosmic microwave background radiation [14]. The comparison of the baryonic density inferred from BBN and cosmic microwave background constitutes a fundamental test of big-bang cosmology.

The latest BBN network calculations [16] used theoretical predictions [17,18] rather than a fit to the limited experimental  $pn \rightarrow d\gamma$  cross section data. Theoretical uncertainties are claimed to be small, but some discrepancies remain [19]. Experimentally, attempts have been made to extract the spin flip  $M1$  response in charge-exchange reactions, but presently quantitative results are limited by insufficient energy resolution [20] and the complex reaction mechanism [20,21]. Alternatively, measurements of the analyzing power in the  $\gamma d \rightarrow pn$  reaction provide the  $M1/E1$  ratio [22], but the  $M1$  strength can again be extracted with the aid of theory only. Here we present a study of the  ${}^2\text{H}(e, e')$  reaction under  $180^\circ$  with good energy resolution sufficient to map the  $M1$  resonance. The kinematics ensures a selective excitation of the  $M1$  strength. The impact on an improved description of the  $pn \rightarrow d\gamma$  reaction is twofold: these data serve as a stringent test of the above-mentioned theoretical approaches at finite momentum transfer and furthermore—by extrapolation to the photon point—provide the first set of data fully covering the energy region relevant to BBN. With reasonable approximations [23], the transverse electromagnetic response measured in the present work can also be related to the generalized Gerasimov-Drell-Hearn sum rule for deuteron electrodisintegration [24].

The experiment was performed at the  $180^\circ$  electron scattering facility [25] of the superconducting Darmstadt electron linear accelerator S-DALINAC coupled to a high-resolution, large solid-angle magnetic spectrometer of clamshell type [26]. The measurements were done at incident energies  $E_0 = 27.8$  and  $74.0$  MeV, corresponding to momentum transfers  $q = 0.27$  and  $0.74 \text{ fm}^{-1}$  at the breakup threshold, respectively. Targets consisted of deuterated polyethylene  $[(\text{C}_2\text{D}_4)_n]$  with thicknesses between  $4.8$  and  $9.6 \text{ mg/cm}^2$ . Typical beam currents were

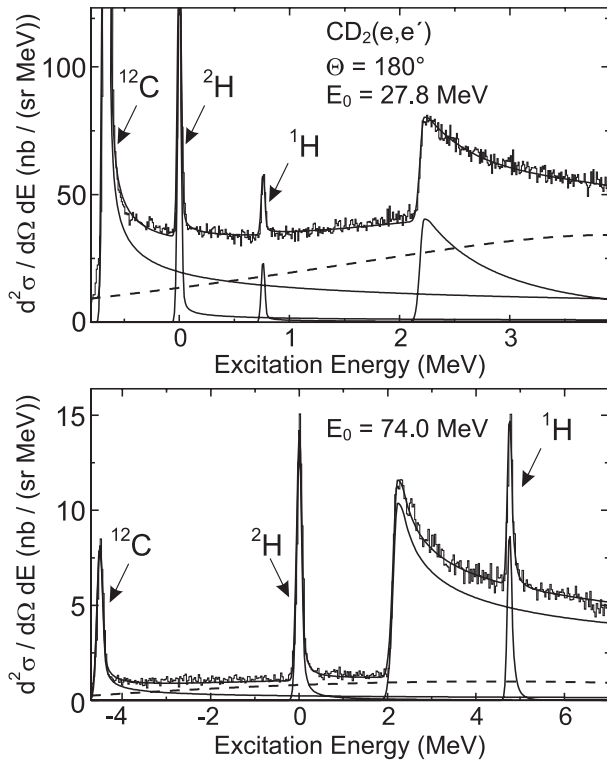


FIG. 1. Spectra of the  $(e, e')$  reaction on deuterated polyethylene at  $E_0 = 27.8$  and  $74.0$  MeV and  $\Theta = 180^\circ$  and their decomposition into elastic scattering from  $^1\text{H}$ ,  $^2\text{H}$ , and  $^{12}\text{C}$  and deuteron breakup (solid lines) and instrumental background (dashed lines).

100–250 nA. To avoid evaporation due to the heat load, the targets were mounted on a wobbling system [27].

The resulting spectra are displayed in Fig. 1. The magnetic spectrometer settings were chosen to include the elastic scattering peaks of  $^{12}\text{C}$ ,  $^2\text{H}$ , and  $^1\text{H}$ . The breakup cross sections could be measured up to 4 MeV at the lower and up to 7 MeV at the higher momentum transfer. Decompositions into contributions from the elastic scattering peaks with a line shape described in [28] and the deuteron breakup (solid lines) and an instrumental background (dashed lines) are also shown. The latter was determined from measurements with an empty target frame. Energy resolutions of 45 and 140 keV (full width at half maximum) were achieved at the lower and higher incident electron energy, respectively.

Absolute cross sections were determined in two independent ways. On the one hand, they were calculated from the experimental target and spectrometer parameters and the total collected charge. Alternatively, the experimental counting rates were normalized relative to the structure functions  $A(q^2)$  and  $B(q^2)$  of the elastic scattering cross sections, resulting from the interaction of the scattered electron with the nuclear charge and magnetization distributions inside the deuteron, respectively. A summary of data [29–32] at momentum transfers below  $q^2 = 2 \text{ fm}^{-2}$  is presented in Fig. 2 together with an empirical fit. The

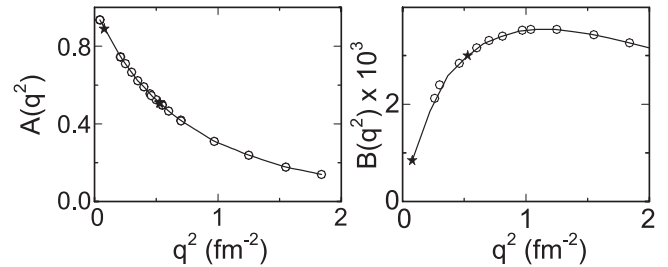


FIG. 2. Data (open circles) for the structure functions  $A(q^2)$  [29,30] and  $B(q^2)$  [30–32] of elastic electron-deuteron scattering. Present results are shown as stars. The solid lines are polynomial fits to the data.

present results, indicated by stars, are in excellent agreement with this parametrization. The agreement between the two methods is better than 6% for both the spectra.

In order to extract the breakup cross sections, the response function had to be unfolded from the data. This was achieved applying either Tikhonov’s method or Fourier transforms as described, e.g., in [33] leading to identical results. The unfolded spectra are shown in Fig. 3, where the hatched areas indicate the experimental uncertainties of the cross sections (note that the analysis was performed for 10 keV bins but smoothed curves are plotted for better visibility). We also include the uncertainty in the excitation energy determination ( $\pm 10$  keV).

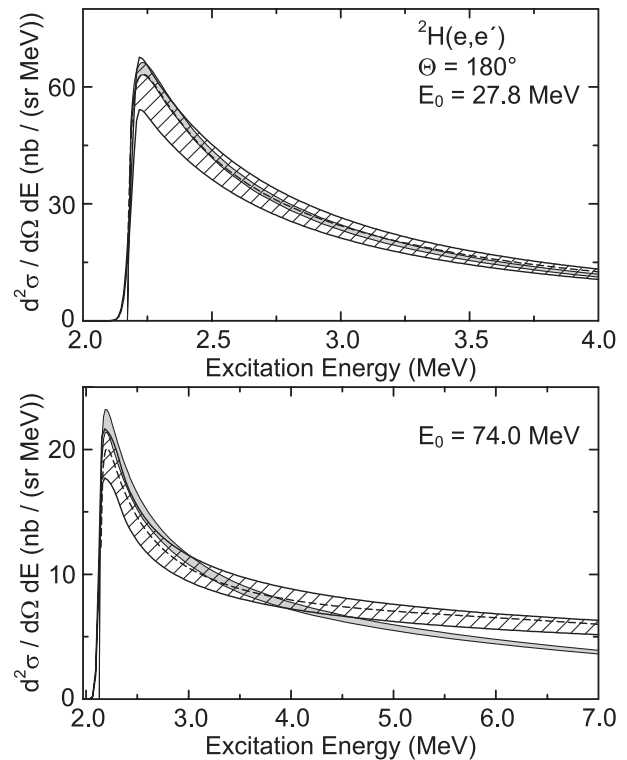


FIG. 3. Double-differential cross sections of the  $^2\text{H}(e, e')$  reaction with errors (hatched bands) extracted from the spectra of Fig. 1. The gray bands and dashed lines are EFT (hatched) and potential model calculations, respectively, explained in the text.

We now discuss theoretical approaches to describe the data based on the potential model and EFT( $\not{\hbar}$ ) calculations, respectively. In the former, the longitudinal and transversal inelastic form factors, which govern the inclusive cross sections, are calculated within a nonrelativistic framework. The initial and final state wave functions are obtained by solving the two-body Schrödinger equation with a realistic  $NN$  potential for the bound and the scattering states as well. The calculation uses the Argonne high-precision  $V_{18}$  potential [34]. The leading current contribution is provided by the nonrelativistic one-body nucleon current. In addition, we consider subnuclear degrees of freedom related to meson exchange currents and isobar configurations and, furthermore, relativistic contributions of leading order beyond the nonrelativistic current [35]. Details may be found in Ref. [2].

The EFT calculation uses the variant in which the effective range is resummed into the two-nucleon propagator [36]. The amplitude is expanded in a dimensionless parameter determined by the ratio of the inverse  $NN$ -scattering lengths or the momentum of the virtual photon to the inverse range of the pion-exchange potential (the pion mass). This allows to estimate theoretical uncertainties of the calculation induced by neglecting higher-order terms in the momentum expansion of all forces. The low-energy data set at  $q = 0.27 \text{ fm}^{-1}$  lies well within the range of applicability of EFT( $\not{\hbar}$ ), while the expansion breaks down for the higher-energy data where  $q = 0.74 \text{ fm}^{-1} \approx m_{\pi}c/\hbar$ ; i.e., it roughly corresponds to the range of pion exchange and thus at best qualitative agreement with experiment can be expected.

The description of deuteron electrodisintegration in this framework has been discussed by Christlmeier and Griebhammer [37], which resolved also discrepancies between theory and earlier exclusive  ${}^2\text{H}(e, e'p)n$  experiments [38]. The  $E1$  amplitude follows up to next-to-next-to-leading order from minimal substitution of all derivatives in the  $NN$  Lagrangian. It is determined by the scattering lengths and effective ranges of singlet and triplet  $S$ -wave scattering and by the deuteron quadrupole moment. For  $M1$  transitions, the photon couples in leading order to the nucleonic magnetic moment. The only new interaction at next-to-leading order couples a magnetic photon to a transition operator between triplet and singlet  $S$ -wave states of  $NN$  scattering. Different methods to determine its strength from the total thermal  $np \rightarrow d\gamma$  cross section [39] give an estimate of the theoretical uncertainties of this universal approach; see [37] for details.

A comparison of the potential model and EFT( $\not{\hbar}$ ) predictions with the data is shown in Fig. 3. At the lower momentum transfer, excellent agreement between the experimental and theoretical results is obtained. The small differences at the maximum of the breakup peak are within the experimental uncertainties and the accuracy of the EFT( $\not{\hbar}$ ) calculation, as mentioned above. At higher  $q$ , the data are again described by the potential model calculations; the EFT( $\not{\hbar}$ ) results are in reasonable agreement at

low excitation energies but underestimate the data at higher excitation energies.

In the next step we extrapolate our data to the photon point to extract the cross sections of the  $\gamma d \rightarrow pn$  reaction. By the principle of detailed balance this also determines the initial  $pn \rightarrow d\gamma$  fusion reaction in BBN. However, because of the direct relation to the electron scattering data, it is more convenient to discuss the results in terms of photoinduced deuteron breakup. The  $q$  dependence deduced for the transverse structure function of elastic deuteron scattering shown in Fig. 2 is assumed for the extraction of the equivalent real photon cross sections. The validity of this approach can be checked by analyzing the cross section ratio of the two spectra, which should then be constant; this is well fulfilled for excitation energies up to 3 MeV.

The upper part of Fig. 4 summarizes all available data for photoinduced deuteron breakup at energies close to the threshold [7–11]. We also include the  $pn \rightarrow d\gamma$  results [6] using detailed balance. The solid line represents both the potential model and the EFT( $\not{\hbar}$ ) calculations [40], which

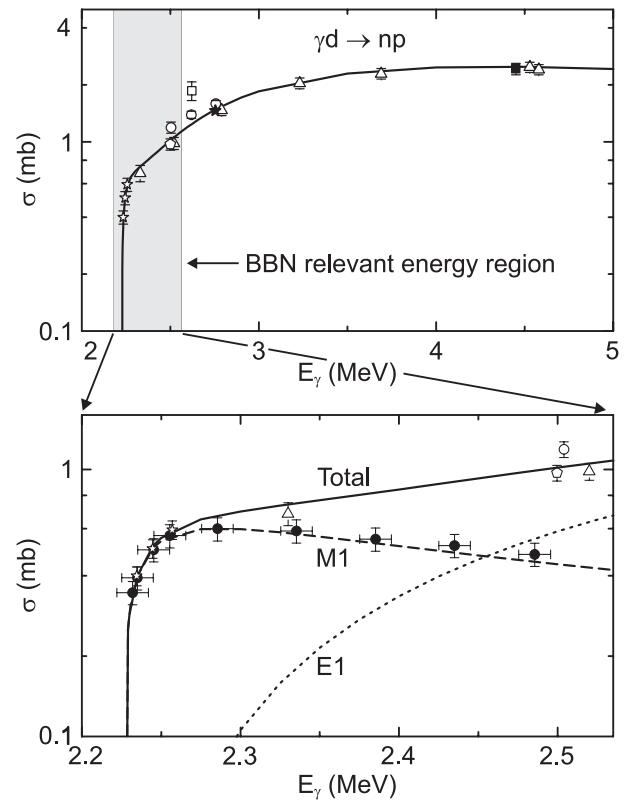


FIG. 4. Top: Total cross section of the  $\gamma d \rightarrow pn$  reaction. Data are from [6] (open stars), [7] (open square), [8] (open circles), [9] (solid squares), [10] (solid star), and [11] (open triangles). Bottom: cross sections deduced from the present experiment (solid dots) in the BBN energy regime. The error bars correspond to the uncertainties of the cross section and energy determination. The model results are decomposed into  $M1$  and  $E1$  parts. Potential model and EFT( $\not{\hbar}$ ) calculations (solid, dashed, and dotted lines) agree within line thickness.

are indistinguishable within line thickness (differences are  $<2\%$  at all energies). Good overall agreement is obtained, but the few data in and close to the energy region relevant to BBN (marked in gray) show considerable scattering.

The photon energy region relevant to BBN is expanded in the lower part of Fig. 4. The present results are included as full circles. For the first time, one has a consistent data set covering the full temperature range of BBN with good energy resolution, including the steep slope at threshold and the peak region of the spin flip  $M1$  resonance. Because of the enhancement of transverse cross sections in  $180^\circ$  electron scattering, the  $M1$  part of the total cross sections is selectively excited. This provides an accurate approximation to the full cross sections in the region of the spin flip  $M1$  resonance, but  $E1$  contributions are non-negligible toward higher energies. A decomposition of the potential model and EFT( $\not\hbar$ ) approaches into  $M1$  and  $E1$  parts demonstrates again perfect agreement with the present data.

To summarize, the deuteron breakup close to threshold has been studied in  $180^\circ$  electron scattering at low momentum transfers with good energy resolution. This allows one to map in detail the spin flip  $M1$  response, which dominates the  $pn \rightarrow d\gamma$  reaction over the BBN temperature region. Potential model calculations and (in the range of applicability) results from pionless EFT( $\not\hbar$ ) are in excellent agreement with the data and should thus provide reliable  $pn \rightarrow d\gamma$  cross sections for BBN network calculations.

The experiment originated from a discussion of one of us (A.R.) with G. A. Peterson. We are grateful to him and also to H. R. Weller for discussions and to S. Christlmeier for his contributions to the EFT( $\not\hbar$ ) calculations. We acknowledge H.-D. Gräf and the S-DALINAC team for preparing excellent beams. This work was supported by the DFG under Contract No. SFB 634 and in part (H.A.) under Contract No. SFB 443. H.W.G. was supported in part by the BMBF, by the DFG under Contracts No. GR1887/2-2 and No. 3-1, by a NSF CAREER grant No. PHY-0645498, and by a DOE grant No. DE-FG02-95ER-40907. B.Ö. and S.R. received financial support from the DAAD.

\*Present address: DESY, D-15738 Zeuthen, Germany.

†vnc@ikp.tu-darmstadt.de

- [1] R. Gilman and F. Gross, *J. Phys. G* **28**, R37 (2002).
- [2] H. Arenhövel, W. Leidemann, and E.L. Tomusiak, *Eur. Phys. J. A* **23**, 147 (2005).
- [3] P.F. Bedaque and U. van Kolck, *Annu. Rev. Nucl. Part. Sci.* **52**, 339 (2002).

- [4] E. Epelbaum, *Prog. Part. Nucl. Phys.* **57**, 654 (2006).
- [5] S. Burles *et al.*, *Phys. Rev. Lett.* **82**, 4176 (1999).
- [6] T. S. Suzuki *et al.*, *Astrophys. J.* **439**, L59 (1995); Y. Nagai *et al.*, *Phys. Rev. C* **56**, 3173 (1997).
- [7] K. Shinohara, T. Okada, and S. Morita, *J. Phys. Soc. Jpn.* **4**, 77 (1949).
- [8] G.R. Bishop *et al.*, *Phys. Rev.* **80**, 211 (1950).
- [9] C.A. Barnes *et al.*, *Phys. Rev.* **86**, 359 (1952).
- [10] R. Moreh, T. J. Kennett, and W. V. Prestwich, *Phys. Rev. C* **39**, 1247 (1989).
- [11] K. Y. Hara *et al.*, *Phys. Rev. D* **68**, 072001 (2003).
- [12] K.M. Nollett and S. Burles, *Phys. Rev. D* **61**, 123505 (2000).
- [13] R.H. Cyburt, *Phys. Rev. D* **70**, 023505 (2004).
- [14] D.N. Spergel *et al.* (WMAP), *Astrophys. J. Suppl. Ser.* **170**, 377 (2007).
- [15] D.N. Schramm and M. S. Turner, *Rev. Mod. Phys.* **70**, 303 (1998).
- [16] A. Coc *et al.*, *Astrophys. J.* **600**, 544 (2004).
- [17] J.-W. Chen and M.J. Savage, *Phys. Rev. C* **60**, 065205 (1999).
- [18] G. Rupak, *Nucl. Phys. A* **678**, 405 (2000).
- [19] S. Ando *et al.*, *Phys. Rev. C* **74**, 025809 (2006).
- [20] S. Nakayama *et al.*, *Phys. Rev. C* **72**, 041001(R) (2005).
- [21] C. Bäumer *et al.*, *Phys. Rev. C* **71**, 044003 (2005).
- [22] E. C. Schreiber *et al.*, *Phys. Rev. C* **61**, 061604(R) (2000); W. Tornow *et al.*, *Phys. Lett. B* **574**, 8 (2003).
- [23] H.R. Weller and M. W. Ahmed, *Mod. Phys. Lett. A* **18**, 1569 (2003).
- [24] H. Arenhövel, *Phys. Lett. B* **595**, 223 (2004).
- [25] C. Lüttge *et al.*, *Nucl. Instrum. Methods Phys. Res., Sect. A* **366**, 325 (1995).
- [26] H. Diesener *et al.*, *Phys. Rev. Lett.* **72**, 1994 (1994).
- [27] D. Hoffmann *et al.*, *Nucl. Instrum. Methods* **118**, 321 (1974).
- [28] F. Hofmann *et al.*, *Phys. Rev. C* **65**, 024311 (2002).
- [29] G. G. Simon, C. Schmitt, and V. H. Walther, *Nucl. Phys. A* **364**, 285 (1981).
- [30] S. Platchkov *et al.*, *Nucl. Phys. A* **510**, 740 (1990).
- [31] J. Goldemberg and C. Schaerf, *Phys. Rev. Lett.* **12**, 298 (1964).
- [32] E. C. Jones *et al.*, *Phys. Rev. C* **21**, 1162 (1980).
- [33] F. Beck *et al.*, *Phys. Lett. B* **645**, 128 (2007).
- [34] R. W. Wiringa, V. G. J. Stoks, and R. Schiavilla, *Phys. Rev. C* **51**, 38 (1995).
- [35] F. Ritz *et al.*, *Phys. Rev. C* **55**, 2214 (1997).
- [36] S.R. Beane and M.J. Savage, *Nucl. Phys. A* **694**, 511 (2001).
- [37] S. Christlmeier and H. Griebhammer, arXiv:0803.1307.
- [38] P. von Neumann-Cosel *et al.*, *Phys. Rev. Lett.* **88**, 202304 (2002).
- [39] A.E. Cox, S.A.R. Wynchank, and C.H. Collie, *Nucl. Phys.* **74**, 497 (1965).
- [40] This result was first derived in Ref. [36].